Study of the reducibility of Pt or Pd on ceria–zirconia catalysts by XANES measured at the Ce L$_{III}$ edge and magnetic susceptibility measurements

Aaron Norman[a], Vincent Perrichon[a,*], Abdeltif Bensaddik[b], Sylvain Lemaux[b], Harry Bitter[b]
and Diek Koningsberger[b]

[a] *Laboratoire d'Application de la Chimie à l'Environnement (LACE), UMR 5634 CNRS, Université Claude Bernard Lyon 1,*
43 boulevard du 11 Novembre 1918, 69622 Villeurbanne Cedex, France
E-mail: Vincent.Perrichon@univ-lyon1.fr

[b] *Department of Inorganic Chemistry University of Utrecht, Sorbonnelaan 16, PO Box 80083, 3508 TB, Utrecht, The Netherlands*

The reduction behaviour of Ce$_x$Zr$_{1-x}$O$_2$ and Pt or Pd supported on Ce$_x$Zr$_{1-x}$O$_2$ was investigated by means of XANES measured at the Ce L$_{III}$ edge and magnetic susceptibility measurements. Both techniques agree quite closely for the materials studied. The presence of a noble metal greatly improves the reduction of the Ce$_x$Zr$_{1-x}$O$_2$ support at low temperatures. The reoxidation that occurred after evacuation of the reduced solids and heating to 500 °C suggests that it is linked to a reversible surface reduction process of the sample.

KEY WORDS: ceria–zirconia; palladium catalyst; platinum catalyst; reduction by H$_2$; ceria redox properties; XANES; magnetic study

1. Introduction

The wide use of ceria as a promoter in three-way automotive catalysis for emission control is due to its ability to store and release oxygen, as required, during the catalytic degradation of pollutants [1–3]. The most significant problem encountered when using ceria is the decrease in the oxygen storage capacity (OSC) under normal driving conditions [4] which is further aggravated by the use of close-coupled catalysts in order to overcome cold start-up problems [5]. The incorporation of ZrO$_2$ into the CeO$_2$ lattice benefits the material two-fold by both stabilising the surface area of the mixed oxide system and by allowing a greater reduction of the ceria due to oxygen vacancy migration into the bulk of the material resulting in better OSC properties [4,5]. This resulted in a new generation of automotive exhaust three-way catalysts using ceria–zirconia mixed oxides, Ce$_x$Zr$_{1-x}$O$_2$, instead of pure ceria as a support for the catalytically active noble metals (NM). The reduction/oxidation behaviour, which is believed to be closely related to the oxygen storage capacity of these materials is now well documented [4,6–11]. However, the oxides impregnated with NM certainly require more study, particularly concerning their redox and chemisorptive behaviour. This work reports on the reducibility and the redox behaviour of these noble-metals-containing materials using XANES measured at the Ce L$_{III}$ edge and magnetic susceptibility measurements. Both techniques give information on the bulk reduction of the materials and allow *in situ* measurements.

* To whom correspondence should be addressed.

2. Experimental

2.1. Materials

All materials were provided by Rhodia (CEZIRENCAT samples). They were of a high surface area (HS ≈ 100 m^2 g^{-1}). In addition to ceria, two mixed oxides with the composition Ce$_{0.68}$Zr$_{0.32}$O$_2$ and Ce$_{0.50}$Zr$_{0.50}$O$_2$ were studied. Noble metals were impregnated onto the oxide using Pt(NH$_3$)$_4$(OH)$_2$ or Pd(NH$_3$)$_4$(NO$_3$)$_2$ as chlorine free precursors. The metal content was ∼0.5 wt%. Samples are designated a code NM CZ X/100-X, where NM is Pt or Pd and X is the cerium molar composition in the oxide (in %). If no NM is mentioned, the sample is the mixed oxide only.

2.2. XANES (X-ray absorption near-edge spectroscopy)

XAFS data were measured at the ESRF in Grenoble (France) at the BM01. The beamline was equipped with a channel cut (111) monochromator. Harmonic rejection, by decreasing the intensity to 50%, was performed by using a curved Cr mirror. All measurements were performed at liquid nitrogen temperature after the sample was given an *in situ* treatment as required. The detectors were ionisation chambers filled with He/Ar mixtures. The resolution of the experiment could be estimated to about 0.5 eV.

The XANES region of the Ce L$_{III}$ edge can be used to calculate the reduction percentage of ceria as different features exist for each of the two different oxidation states. This difference is illustrated by the spectra of Ce(NO$_3$)$_3$ and CeO$_2$ which are shown in figure 1. Only one peak (peak B$_0$) is observed for Ce^{3+}, whereas Ce^{4+} shows two features (peaks B$_1$ and C). The features observed in the Ce L$_{III}$ edge have been assigned previously [12–14]. These differences were
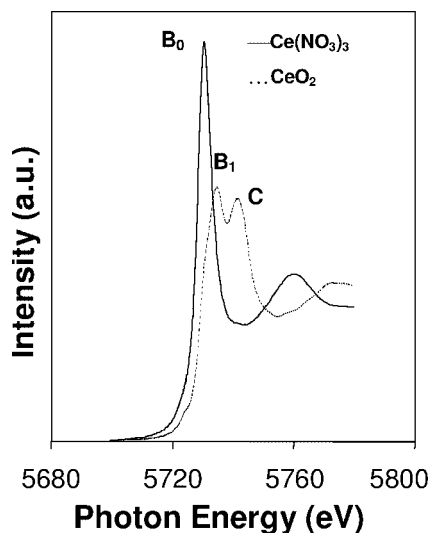
Figure 1. Reference XANES spectra: Ce L_{III} edge of CeO_2 (Ce^{4+}) and $Ce(NO_3)_3$ (Ce^{3+}).
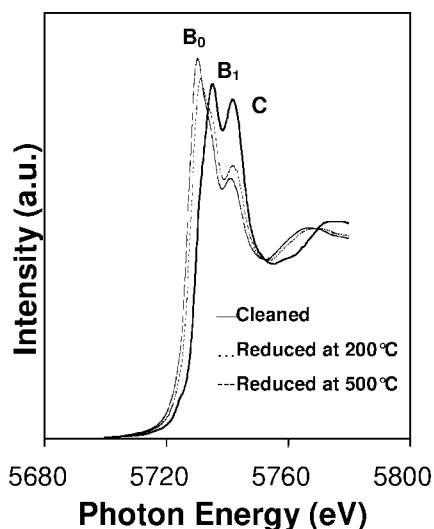

Figure 2. Pd CZ 50/50 sample: normalisation of the spectra at 50 eV above the edge.

used to extract the degree of cerium reduction (% of Ce^{3+}) using different approaches [12,15]. The analysis procedure described by Overbury [15] has been adopted here.

The pre-edge of the obtained data was subtracted by using a modified Victoreen function. The background of the thus obtained spectra was subtracted using a cubic spline function. All data handling was performed using the XDAP program [16]. Next the spectra were normalised at 50 eV above the edge. Figure 2 shows, as an example, the spectra for Pd CZ 50/50 after this processing. The spectrum of the cleaned sample was assumed to be representative for that of a sample in which the Ce is fully oxidised and was used as a reference. This fully oxidised spectrum is then subtracted from the spectra obtained after reduction at 200 and 500 °C, and from the untreated sample thus obtaining a difference spectrum for each temperature. The extent of reduction is directly related to the negative increase of the height of peak C

and the positive increase of the B_0 peak (i.e., the difference in intensity between the both peaks) as shown in the difference curves (see figure 5). The calibration of the extent of reduction was made using the same procedure on $Ce(NO_3)_3$ and CeO_2, chosen as references of a fully reduced sample (100% of Ce^{3+}) and a fully oxidised sample (100% Ce^{4+}). The precision of the procedure was estimated using physical mixtures of Ce^{3+} and Ce^{4+} with a known Ce^{3+}/Ce^{4+} ratio. When performing the analysis procedure as described above, we obtained ratios which were accurate within 10%.

2.3. Magnetic balance (MB)

Magnetic susceptibility measurements were carried out on a Faraday microbalance. The experimental set-up and procedure for calculation of the magnetic susceptibilities have been described elsewhere [17,18]. The method allows the determination of the paramagnetic Ce^{3+} content. All samples were submitted to a series of reduction treatments at various temperatures under 5% H_2/He, as detailed below. Magnetic susceptibility measurements were performed at 25 °C before and after all temperature treatments and atmospheric changes.

2.4. Protocol

A standard protocol for testing and analysing CEZIREN-CAT samples was established within that project. All samples were subjected to a cleaning pre-treatment in order to have an equivalent starting point for the two techniques used [19]. This consisted of a heating step in 5% O_2/He at atmospheric pressure, to 550 °C for 1 h (all heating and cooling rates were 10 °C/min). After cooling, the system was evacuated and the system reheated to 500 °C and left at that temperature for 1 h. This procedure generally gave results of ∼1–2% of Ce^{3+}.

The next step consisted of the introduction of 5% H_2/He to the sample at RT for chemisorptive studies. The protocol allowed for times of up to 24 h of equilibration in the MB, in order to attain a steady state. This extended time was to determine the RT activity of the material. After all heat treatments and changes of atmosphere 15 min of equilibration was allowed to obtain a pseudo equilibrium state. All further treatments consisted of the introduction of flowing 5% H_2/He and heating to the reduction temperature for 1 h. After cooling, the quantity of Ce^{3+} was measured, then the system was evacuated and heated to the same temperature for 1 h. A measurement of the Ce^{3+} was performed again after cooling, and then if the reduction temperature was less than 500 °C the system was heated to 500 °C for 1 h prior to another measurement. In this way we were able to obtain three distinct characteristics of reduction at each temperature:

(i) the "total reduction" corresponding to the Ce^{3+} extent obtained after reduction under H_2;

(ii) the "irreversible reduction" obtained after evacuation at RT and subsequent heating to the reduction temperature

and 500 °C (if the reduction temperature is less than 500 °C);

(iii) the "redox reversibility" which is the difference between total and irreversible reduction.

The protocol for the XANES studies was similar but a little simplified. It consisted of this H$_2$ chemisorption for one hour at 25, 200, 350 and 500 °C, whereas the MB also used intermediate temperatures with reduction at 100, 275 and 425 °C, and the higher temperatures of 600 and 700 °C. Due to these inherent differences in protocol for both techniques some variations are to be expected on the reduction extents.

3. Results and discussion

3.1. Reduction of Ce$_{0.68}$Zr$_{0.32}$O$_2$ and Ce$_{0.50}$Zr$_{0.50}$O$_2$: comparison between both techniques

In order to test the comparability of both techniques the reduction degree of the ceria–zirconia mixed oxide supports, reduced at 200 and 500 °C in flowing 5% H$_2$/He was investigated by both the magnetic balance and XANES. Table 1 gives the extent of reduction defined as the ratio Ce^{3+}/(Ce^{3+} + Ce^{4+}). It can be clearly seen that both techniques give extremely comparable results for these samples and can therefore be used to study the reducibility and the reversible reduction of the NM-loaded CZ materials. Results

Table 1
Comparison of the total reduction of ceria–zirconia mixed oxides using XANES and magnetic susceptibility measurements.

Sample	Temperature (°C)	Atmosphere	XANES (%)	Magnetic balance (%)
CZ 68/32 HS	500	H$_2$	40.0	44.7
CZ 50/50 HS	200	H$_2$	<5	2.7
	500	H$_2$	56.7	56.2

in table 1 also confirm those obtained previously on ceria–zirconia mixed oxides [7–10].

3.2. Influence of platinum and palladium on the reduction of Ce$_{0.68}$Zr$_{0.32}$O$_2$

Figure 3 shows the MB results obtained for CZ 68/32 HS, both in the presence and absence of a NM. Results are plotted as mmol Ce^{3+} present per g catalyst versus reduction temperature. It can be clearly seen from this figure that the noble metal enhances the low temperature reduction of Ce. In the case of Pd a reduction is already observed at RT whereas for Pt the reduction of Ce starts between 100 and 200 °C. Note that in the absence of a NM the reduction starts only at 300 °C. Figure 3 also shows that Pd and Pt give similar extents of reduction at high temperature. The reduction extent at 700 °C reaches approximately 3.0 mmol-Ce^{3+} g-cat^{-1}. This equates to about 75% of the ceria being reduced, a value not too far from that obtained with the CZ 68/32 oxide alone (65%). These results confirm those reported on Rh/Ce$_x$Zr$_{1-x}$O$_2$ [15].

On the basis of previous observations and conclusions made on the reduction by hydrogen of noble metals supported on ceria [20–22] and on ceria–zirconia [23,24], we can consider that reduction of the redox support takes place via two competing mechanisms: (i) at low temperatures, H$_2$ is dissociated in the presence of a NM according to H$_2$ → 2H˙. Spillover occurs and this results in the formation of OH species, which causes the Ce to exist as the trivalent cation. This has been shown to be a surface associated reaction exhibiting a high degree of reversibility via a back spillover mechanism [25] (ii) at high temperatures, the creation of oxygen vacancies is favoured. This is caused by the loss of water from the surface of the material leaving an oxygen vacancy associated with Ce^{3+} cations. Bulk oxygen then migrates to the surface to replace the lost oxygen, effectively causing the oxygen vacancy to migrate to the bulk. This corresponds to an irreversible process.
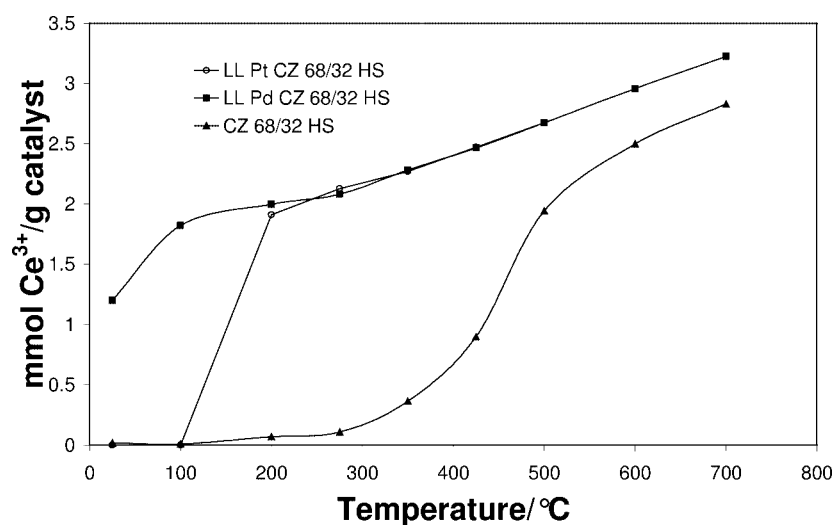

Figure 3. Ce^{3+} concentration versus reduction temperature for CZ 68/32 HS, Pd CZ 68/32 HS and Pt CZ 68/32 HS. Measurements performed under 5% H$_2$/He. The Ce^{3+} values are given in mmol g-cat^{-1}.

It is important to note here that the reduction at low temperatures of NM/CZ 68/32 HS reduces more Ce ions than present on the surface (about 0.7 mmol g^{-1}). This shows that in the presence of a metal, the bulk oxygen ions of the ceria–zirconia are affected by low temperature reduction. The fact that the reduction of Ce in the Pt-containing sample starts at a higher temperature compared to the Pd-containing sample can be explained by the presence of PtO$_x$ on the surface of the Pt particles, thus inhibiting the spillover as long as reduction in metallic platinum has not occured. Large quantities of oxidised Pt have been detected on the oxidised and reduced ($T < 100\,°C$) samples, but this amount decreases to less than 10% for temperatures of 500 °C and higher [26].

At high temperatures, the second reaction (which essentially is a bulk reaction) becomes predominant, which leads to the supports (Ce–Zr mixed metal oxides) and the NM-impregnated supports (NM Ce–Zr mixed metal oxides) to give similar values. The slightly higher reduction extent of the NM CZ oxides can be attributed to a higher stabilisation of hydroxyl groups when a NM is present. XPS has shown some evidence for the existence of hydroxyls after reduction, evacuation and heating [26]. This point is discussed in section 3.4.

Table 2 summarises some of the MB and XANES results at common reduction temperatures for both techniques. Contrary to the case of the supports alone, it shows a few differences in the data for the NM-impregnated materials. Reduction percentages recorded using the magnetic balance are generally higher than those obtained by XANES. This can be ascribed to differences in the experimental protocol that is in part determined by the individual techniques. The first difference occurs in the RT chemisorption experiments performed on Pd CZ 68/32 HS using the MB. For the MB experiments the sample was exposed to the reducing atmosphere for far longer period (13 h) than for XANES (1 h). This immediately caused higher Ce^{3+} values to oc-

cur. The MB also used intermediate reduction temperatures (not shown in table 2) to obtain more complete data on the process, and these additional steps further elevated the Ce^{3+} concentrations. These effects appear to be additive leading to a difference, after reduction at 500 °C, of about 10% for Pd CZ 68/32 HS and Pt CZ 68/32 HS. Despite these differences both techniques show that the addition of a NM to the oxides increases the efficiency of the reduction process (see table 1 for comparison).

3.3. Influence of the composition of the mixed oxide on the reduction of NM–Ce$_x$Zr$_{1-x}$O$_2$

The reducibility of the mixed oxides, with and without Pd, is seen in figure 4. As in figure 3, results are plotted as mmol-Ce^{3+} g^{-1} to allow the direct comparison of materials of different composition. When the reduction behaviour of the pure CeO$_2$ sample is compared to those where Zr is present it is clear that in the Zr-containing samples more Ce^{3+} is present. Thus Zr assists in the reduction of the lattice as a whole in agreement with previous works [7–10].

When palladium is deposited on the oxides, again there is an improvement of the reducibility at low temperature, confirming the occurrence of hydrogen spillover, but with a

Table 2
Comparison of the degree of reduction of NM impregnated ceria–zirconia, under H$_2$ at 200 and 500 °C, using XANES and magnetic susceptibility measurements.

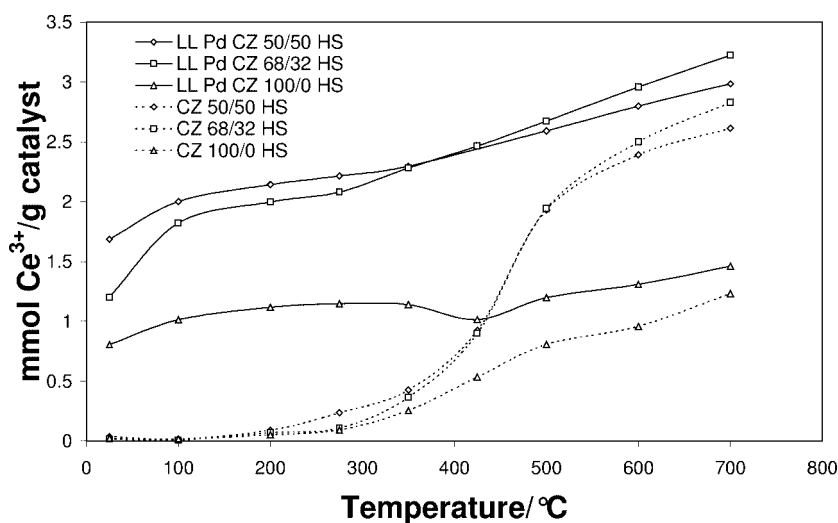| Sample	Temperature (°C)	Atmosphere	XANES (%)	Magnetic balance (%)
Pd CZ 68/32 HS	25	H$_2$	7.2	27.6 (13 h)
	200	H$_2$	43.3	46.0
	200	Vacuum	15.4	30.5
	500	Vacuum	21.5	25.2
	500	H$_2$	52.7	61.5
	500	Vacuum	33.1	44.5
Pt CZ 68/32 HS	200	H$_2$	44.5	44.0
	500	H$_2$	51.7	61.6

Figure 4. Ce^{3+} concentration versus reduction temperature for Pd CZ 100/0 HS, Pd CZ 68/32 HS and Pd CZ 50/50 HS compared to the support alone. Ce^{3+} values given in mmol g-cat^{-1}.
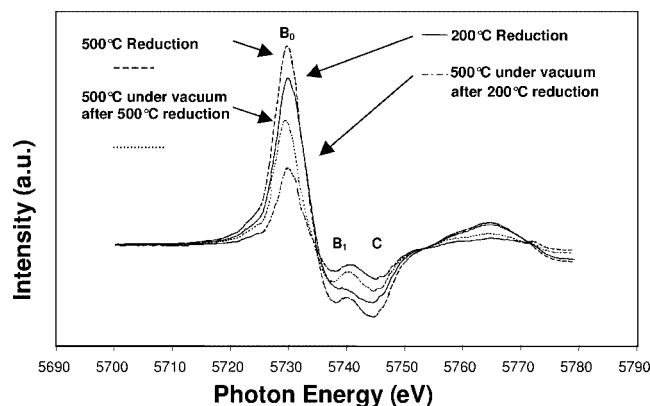
Figure 5. Reversibility of the reduction evidenced by XANES on the Pd CZ 68/32 HS catalyst. The difference spectra are obtained by subtraction of the spectrum of the fully oxidised sample (100% Ce^{4+}) from the spectra of the reduced spectra.

Table 3
Reversibility data for the Pd CZ 68/32 HS catalyst (deduced from table 2).

Sample	Temperature (°C)	XANES (%)	Magnetic balance (%)
Pd CZ 68/32 HS	200	21.8	20.8
	500	19.6	17.0

distinct difference between ceria and the two ceria–zirconia oxides. As shown in figure 4, the extent of reduction for Pd CZ 100/0 HS remains close to that of the surface reduction only, i.e., ~1 mmol-Ce^{3+} g-cat^{-1} [27]. For the NM–Ce$_x$Zr$_{1-x}$O$_2$, the Ce^{3+} concentration at low temperature is at least twice that of the pure ceria material, giving evidence that the bulk reduction effectively occurs in this low temperature range. XANES measurements performed on the Pd CZ 50/50 HS sample confirm these results, with however a difference of over 15% observed with the MB which again can be explained by a much higher Ce^{3+} value obtained in the MB after 9.5 h under hydrogen at 25 °C.

3.4. Reversibility of the reduction of the materials

Reversible reduction has been defined as the difference between the reduction levels after treatment in H$_2$ at the reduction temperature and after subsequent heating of the material in vacuum at 500 °C. This difference is thought to be the reduction that corresponds to the presence of OH species adsorbed on cerium ions, very likely hydroxy groups coordinated to two cations in the proximity of an oxygen vacancy [28]. For ceria and ceria–zirconia oxides, it has been shown by IR spectroscopy that upon heating in vacuum, these species are eliminated in the range 500–600 °C through hydrogen evolution [29]. At the same time, magnetic susceptibility measurements have shown a slight decrease of the Ce^{3+} content [29]. This reversible H$_2$ adsorption/desorption is also evidenced in the present study and seems favoured by the presence of the noble metal. This can be observed in the XANES as shown in figure 5 for the Pd CZ 68/32 HS sample. Clearly the reoxidation of Ce^{3+} upon evacuation at 500 °C can be observed from the increase of the B$_0$ peak and negative increase of the C peak.

Table 3 shows the values of reversibility for Pd CZ 68/32 HS after reduction at 200 and 500 °C. The results are approximately the same for each technique, with a reversibility value close to ~20%. Since the extent of this reversible reduction is close to the surface reduction percentage, its is suggested that about one layer of hydroxyls can be formed

under H$_2$ and which are stabilised by the presence of the NM. It must be noted that the bare supports do not show significant reversible reduction at 200 °C [29] and only 3–4% after evacuation at 700 °C [30]. This shows the determining effect of the metal on the formation and the stabilisation of OH species on the redox support surface.

4. Summary/conclusions

This work has primarily focussed on the reduction of ceria–zirconia mixed metal oxides that have been impregnated with a NM (NM = Pd, Pt). The similar results for the reduction of the mixed metal oxides without a NM obtained with the MB and XANES showed that both techniques can be used to reliably study the reduction processes on the CZ samples. However, for the NM-impregnated materials there were differences found between the results from each technique. These variances have been explained by the differences in the experimental protocol that were necessary for each of the techniques. Longer periods under a reducing atmosphere and intermediate reduction steps augmented the reduction of the materials studied by magnetic susceptibility measurements. Nevertheless, both techniques showed the same trends.

The addition of a NM to the oxides increases the efficiency of the reduction process of the Ce in the support. The effect is far more obvious at lower temperatures. Reduction occurs at room temperature for the Pd-impregnated materials. The Pt samples, however, do not become reduced until a temperature of 200 °C is reached, i.e., after that PtO$_x$ has been reduced. At higher temperatures, above 500 °C, the results of the supports and the NM-impregnated materials become closer. In fact the irreversible reduction, for the NM-impregnated samples, is almost identical to the pure support. This suggests that at these temperatures formation of oxygen vacancies at the surface is not influenced by the presence of noble metals. The only difference that is seen to exist under hydrogen between the bare support and the NM-impregnated material is thought to be approximately one layer of hydroxyls at the surface, that is maintained by the presence of the NM. This is confirmed by the degree of reduction after heating under vacuum to high temperatures (>500 °C) being close to that of the pure support. It can thus be said that the NM aids the reduction of the ceria zirconia materials at low temperatures, but at high temperatures the only difference is due to the NM stabilised hydroxyl groups present.

Acknowledgement

References

[1] K.C. Taylor, in: *Catalysis, Science and Technology*, Vol. 5, eds. J.R. Anderson and M. Boudart (Springer, Berlin, 1984) p. 119.

[2] R.G. Silver, J.C. Summers and W.B. Williamson, Stud. Surf. Sci. Catal. 71 (1991) 167.

[3] A. Trovarelli, Catal. Rev. Sci. Eng. 38 (1996) 439.

[4] J. Kaspar, P. Fornasiero and M. Graziani, Catal. Today 50 (1999) 285.

[5] J.P. Cuif, G. Blanchard, O. Touret, M. Marczi and E. Quéméré, SAE 970463.

[6] G. Ranga Rao, P. Fornasiero, R. di Monte, J. Kaspar, G. Vlaic, G. Balducci, S. Meriani, G. Gubitosa, A. Cremona and M. Graziani, J. Catal. 162 (1996) 1.

[7] P. Fornasiero, G. Balducci, R. di Monte, J. Kaspar, V. Sergo, G. Gubitosa, A. Ferrero and M. Graziani, J. Catal. 164 (1996) 173.

[8] P. Fornasiero, E. Fonda, R. di Monte, G. Vlaic, J. Kaspar and M. Graziani, J. Catal. 187 (1999) 177.

[9] E. Finocchio, M. Daturi, C. Binet, J.C. Lavalley, F. Fally, V. Perrichon, H. Vidal, J. Kaspar, M. Graziani and G. Blanchard, Stud. Surf. Sci. Catal. 121 (1999) 257.

[10] M. Daturi, E. Finocchio, C. Binet, J.C. Lavalley, F. Fally and V. Perrichon, J. Phys. Chem. B 103 (1999) 4884.

[11] P. Fornasiero, J. Kaspar, V. Sergo and M. Graziani, J. Catal. 182 (1999) 56.

[12] J. El Fallah, S. Boujana, H. Dexpert, A. Kiennemann, J. Majerus, O. Touret, F. Villain and F. Le Normand, J. Phys. Chem. 98 (1994) 5522.

[13] A. Kotani, T. Jo and J.C. Parlebas, Adv. Phys. 37 (1989) 37.

[14] D.D. Beck, T.W. Capehart and R.W. Hoffman, Chem. Phys. Lett. 159 (1989) 207.

[15] S.H. Overbury, D.R. Huntley, D.R. Mullins and G.N. Glavee, Catal. Lett. 51 (1998) 133.

[16] M. Vaarkamp, J.C. Linders and D.C. Koningsberger, Physica B 208/209 (1995) 159.

[17] A. Laachir, V. Perrichon, A. Badri, J. Lamotte, E. Catherine, J.C. Lavalley, J. El Fallah, L. Hilaire, F. Le Normand, E. Quéméré, G.N. Sauvion and O. Touret, J. Chem. Soc. Faraday Trans. 81 (1991) 1601.

[18] J.P. Candy and V. Perrichon, J. Catal. 89 (1984) 93.

[19] M. Daturi, C. Binet, J.C. Lavalley, H. Vidal, J. Kaspar, M. Graziani and G. Blanchard, J. Chim. Phys., Phys. Chim. Biol. 95 (1998) 2048.

[20] S. Bernal, J.J. Calvino, M.A. Cauqui, G.A. Cifredo, A. Jobacho, J.M. Pintado and J.M. Rodriguez-Izquierdo, J. Phys. Chem. 97 (1993) 4118.

[21] A. Bensalem, F. Bozon-Verduraz and V. Perrichon, J. Chem. Soc. Faraday Trans. 91 (1995) 2185.

[22] A. Pfau, J. Sanz, K.D. Schierbaum, W. Göpel, J.P. Belzunegui and J.M. Rojo, Stud. Surf. Sci. Catal. 101 (1996) 931.

[23] P. Fornasiero, J. Kaspar, V. Sergo and M. Graziani, J. Catal. 182 (1999) 56.

[24] F. Fajardie, J.F. Tempère, J.M. Manoli, O. Touret, G. Blanchard and G. Djéga-Mariadassou, J. Catal. 179 (1998) 469.

[25] S. Bernal, J.J. Calvino, G.A. Cifredo, J.M. Rodriguez-Izquierdo, V. Perrichon and A. Laachir, J. Catal. 137 (1992) 1.

[26] A. Norman, R. Sporken, A. Galtayries, F. Mirabella, K. Kenevey, M. Pijolat, R. Baker and S. Bernal, Mater. Res. Soc. Symp. Proc. 581 (2000) 345.

[27] V. Perrichon, A. Laachir, G. Bergeret, R. Fréty, L. Tournayan and O. Touret, J. Chem. Soc. Faraday Trans. 90 (1994) 773.

[28] A. Badri, C. Binet and J.C. Lavalley, J. Chem. Soc. Faraday Trans. 92 (1996) 4669.

[29] M. Daturi, E. Finocchio, C. Binet, J.C. Lavalley, F. Fally and V. Perrichon, J. Phys. Chem. B 103 (1999) 4889.

[30] M. Daturi, E. Finocchio, C. Binet, J.C. Lavalley, F. Fally, V. Perrichon, H. Vidal, N. Hickey and J. Kaspar, J. Phys. Chem. B 104 (2000) 9186.